

NANOMETER-THICK TEXTURED ZnO FILMS: PREPARATION, CHARACTERIZATION AND INTERACTION WITH ETHANOL VAPOR

D. Naumenko,¹ V. Snitka,¹ A. Ulcinas,¹
I. Naumenko,¹ and K. Grigoras²

UDC 546.47+547-311+544.72.05+53.082.531

A study was carried out on the effect of the reaction temperature in atomic layer deposition on the structural and piezoelectric properties of thin ZnO films (5-50 nm) by scanning electron microscopy, X-ray diffraction, piezoresponse force microscopy, and surface acoustic wave (SAW) spectroscopy. The piezoresponse was shown to be mainly a function of ZnO grain size and the monocrystalline structure perpendicular to the substrate plane. The results demonstrate promise for the use of textured ZnO films as sensitive coatings for acoustic gas sensors in instruments based on the SAW transducer amplification-frequency response.

Key words: zinc oxide films, thin films, atomic layer deposition, piezoresponse force microscopy.

Zinc oxide (ZnO) is a unique material with both semiconductor and piezoelectric properties [1-3]. Due to a rather broad forbidden band (3.37 eV), ZnO is commonly used in optoelectronics, photovoltaic devices, and sensor technology, in particular, for radiation recording systems in the ultraviolet spectrum [1, 2]. On the other hand, the lack of a center of symmetry in the ZnO unit cell combined with a high electromechanical coupling coefficient accounts for strong piezo- and pyroelectric properties, which find common use in the manufacture of piezoelectric transducers of mechanical energy, micromanipulators, and devices for the detection of surface acoustic waves [1, 3]. The microscopic piezoelectric properties of a material are a function of the distribution of granules with different orientation on the micro/nanolevel and their total contribution to the piezoresponse. Thus, the study of the local properties of ZnO in the case of thin textured films having mixed orientation of the polycrystalline grains and low unipolarity is important in the investigation of the mechanisms of macroscopic effects and holds practical interest in the preparation of structures with given properties.

Many methods have been reported for preparing ZnO films with micron and submicron thickness such as magnetron spraying, pulsed laser deposition, molecular beam epitaxy, and chemical deposition from the gas phase or solution (see the work of Nagase et al. [4] and the references therein). However, most of these methods yield films with considerable surface roughness and a large scatter in piezoelectric constants. In contrast to the above methods for film preparation, atomic layer deposition (ALD) permits the precise growth of coatings in a broad range of thicknesses, beginning at several nanometers. In the ALD experiment, the sample is placed in a heated reactor and gas precursors are cyclically introduced into the reactor chamber. The ALD process is self-limiting since it is based on consecutive chemical reactions of the gas precursor molecules

¹The Research Center for Microsystems and Nanotechnology, Kaunas University of Technology, Str. Studentu, 65, Kaunas LT-51369, Lithuania. E-mail: denys.naumenko@ktu.lt; vsnitka@ktu.lt.

²VTT Technical Research Center of Finland, P. O. Box 1000, Fi-02044, Finland.

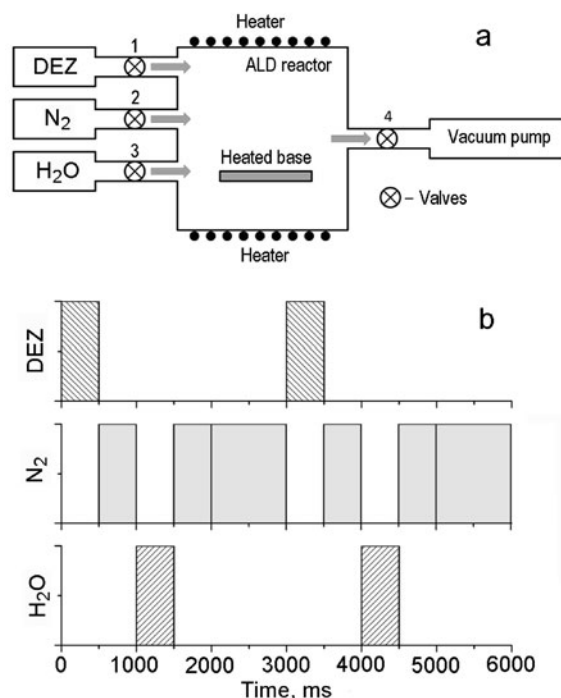


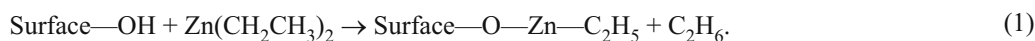
Fig. 1. Simplified scheme of a reactor for atomic layer deposition (a) and timeline for the introduction of the components used into the reactor (b).

with a solid surface, resulting in the layer-by-layer atomic growth of the films on various bases [5]. ALD has a unique advantage in comparison with the other methods for film growth, namely, the possibility of preparing homogeneous coatings on complex 3D objects, including porous materials. In addition, the growth of coatings may be accomplished at rather low reaction temperatures, which opens broad application in optics, biomedical technology, electronics, and nanotechnology [6]. Thus, the study of the physicochemical properties of ALD coatings, including ZnO films, holds enormous present current interest [7]. Furthermore, to the best of our knowledge, there have been no reports concerning the local properties of thin ZnO films grown by ALD.

In the present work, we studied the effect of the temperature of the reaction of atomic layer deposition on the structural, piezoelectric, and functional properties of thin textured ZnO films using scanning electron microscopy (SEM), X-ray diffraction (XRD), piezoresponse force microscopy (PFM), and surface acoustic wave spectroscopy.

The ZnO films were grown by ALD in a Beneq TFS500 reactor (Fig. 1a) at reaction temperatures 165 and 250 °C on bases of crystalline quartz and 100-nm-thick aluminum films deposited on quartz for the PFM measurements. Diethylzinc ($\text{Zn}(\text{CH}_2\text{CH}_3)_2$) and water were used as the precursors, which were introduced consecutively. The exposure time for each component was 500 ms (Fig. 1b). Nitrogen was used as the carrier gas in order to remove residues of $\text{Zn}(\text{CH}_2\text{CH}_3)_2$ or water unreacted on the surface and the reaction products. The carrier gas was introduced into the reaction (over 500 ms) after the inlet of each component and additionally for 1 s at the end of each cycle (Fig. 1b). The number of ALD cycles was set at 250 for each reaction temperature.

The formation of the ZnO films consisted of two intermediate chemical reactions for each of the ALD cycles. In the first step, valve 1 (Fig. 1a) is opened for a given time interval (Fig. 1b) and $\text{Zn}(\text{CH}_2\text{CH}_3)_2$ is introduced into the reactor, where this compound reacts with OH groups adsorbed on the sample surface:



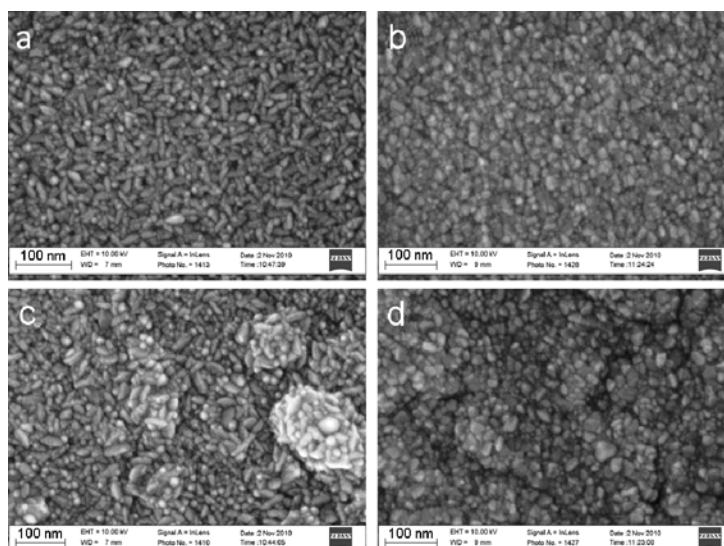
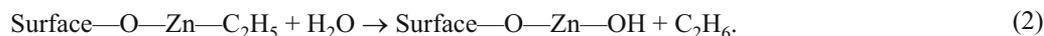


Fig. 2. SEM images of ZnO films on quartz (a, b) and an aluminum film (c, d) grown at the temperatures of the ALD reaction 165 °C (a, c) and 250 °C (b, d).

Valves 2 and 4 (Fig. 1a) are opened during the next pulse (Fig. 1b), such that the residual reaction product (ethane) and excess diethylzinc are removed from the reactor by the gas carrier (in our case, nitrogen).

In the second step, water vapor is introduced into the reactor through valve 3 (Fig. 1a), which reacts with the modified surface:



This reaction product (ethane) and residual water vapor are removed by additional flushing with nitrogen at the end of the cycle (Fig. 1b).

Thus, the total ALD reaction cycle may be described by a single reaction:



while cyclic repetition of this process leads to layer-by-layer atomic growth of the ZnO films in a broad range of thicknesses.

The topography of the grown films (Fig. 2) was studied using a Carl Zeiss SUPRATM40 scanning electron microscope. Figure 2 shows the polycrystalline structure of films with lateral grain dimension of about 20-40 nm, which is in good accord with the data of Jeon [8] and Makino [9]. The films have different orientation of the crystallites relative to the base surface depending on the ALD reaction temperature. However, our study of the surface topography using an atomic force microscope in the intermittent contact (or tapping) mode (these results are not presented) showed that the surface roughness of the films on quartz plates is virtually identical and is 0.92 and 0.94 nm for reaction temperatures 165 and 250 °C, respectively. The general structure of the films for a given number of cycles is invariant in going from quartz to aluminum bases (Fig. 2c,d).

The thickness and refraction index of the ZnO films were calculated from ellipsometric measurements on a Philips instrument ($\lambda = 632.8$ nm) in the single-layer model. We should initially note the greater film thickness by a factor of 1.5 of the film grown at lower temperature. In accord with the generally accepted approach, differences in the growth rate of ALD films and, as a consequence, the film thickness are functions of the ratio between the rate of reaction of the precursors and the probability of the desorption of these compounds from the surface. Desorption begins to predominate with increasing temperature, which is seen in a decrease the film growth rate (Table 1) and is in good accord with literature data [7-9]. On the other hand, the refraction index of the films grown at reaction temperatures 165 or 250 °C is somewhat greater for the films at higher temperature, which indicates denser packing of the film in this case.

TABLE 1. Reaction Temperature, Optical and Electrical Properties of ZnO Films on Quartz Bases Grown by Atomic Layer Deposition (250 cycles)

ALD reaction temperature, °C	Film thickness, Å	Growth rate, Å/cycle	Film refraction index, n	Specific resistance, Ω -cm
165	524 ± 5	2.1	1.948 ± 0.004	0.02
250	342 ± 6	1.4	1.953 ± 0.006	0.01

An X-ray diffraction was carried out on a Philips X'PERT diffractometer ($\lambda = 0.15406$ nm, CuK_α) to check this hypothesis (Fig. 3b). The diameter of the ZnO crystallites calculated using the Rietveld method [10] was 21.6 ± 8.2 and 31.6 ± 12.3 nm for reaction temperatures 165 and 250 °C, respectively. Comparison of these values with the ellipsometric data given in Table 1 shows that the diameter (31.6 ± 12.3 nm) and thickness (34.2 ± 0.6 nm) of the crystallites for the film grown at 250 °C are in good agreement, while these values for the films grown at 165 °C differ by a factor of more than 2 (21.6 ± 8.2 nm vs. 52.4 ± 0.5 nm). This finding suggests that at higher temperature, textured films are formed, whose thickness is not greater than the crystallite diameter, i.e., the film is monocrystalline along the normal to the surface. At the same time at lower temperature the film is polycrystalline in all directions. The electric measurements, in particular, the specific resistance determined by the four-zone method using a Cascade Microtech CPS Keithley 2000 Multimeter qualitatively supports this conclusion: the specific resistance of the film obtained at higher reaction temperature is lower due to a greater amount of the monocrystalline phase and smaller amount of intercrystal barriers (Table 1).

Hence, we find considerable interest in analyzing the local properties of individual crystallites in the film texture. In light of the piezoelectric properties of ZnO, we used piezoresponse force microscopy (PFM) for this purpose. PFM is based on the local action of an external electric field on a piezoelectric sample and the interaction of the probe with the surface of the sample studied. PFM permits the study of the spontaneous polarization of domains and their inversion as well as determination of piezoelectric coefficients at different points on the sample surface [11-13].

The piezoelectric force microscopy was carried out using an NT-MDT SMENA atomic force microscope. An alternating current generator and synchronous amplifier were inserted additionally into the controller. NSG10/TiN commercial conducting probes with modulus of rigidity 20 N/m and curvature radius 35 nm (as indicated by the manufacturer) were used for the PFM measurements. In the PFM mode (see Fig. 3a, insert) between the microconsole, whose probe is in contact with the ZnO film surface, and the lower aluminum electrode, onto which the film is deposited, low-amplitude alternating voltage U_{ac} (0.5 V, 15 kHz) and direct displacement voltage U_{dc} are applied. Local fluctuations of the film thickness (piezoresponse) arise on the frequency of the generator alternating voltage, while departure of the microconsole is detected by the optical system of an atomic force microscope [14]. Upon cyclic change in U_{dc} in a given voltage range, hysteresis loops of the piezoresponse of the films studied may be obtained, as illustrated in Fig. 3a. The ZnO films grown at 250 °C show more pronounced residual polarization, which should also be observed on textured films in contrast to polycrystalline films disoriented along the normal to the film surface.

The X-ray diffraction data show that the diffraction maxima at 31.7° , 34.4° , and 36.2° correspond to crystallographic directions (100), (002), and (101) of hexagonal ZnO [8]. Redistribution of the intensity of the maxima occurs with increasing temperature, which indicates a change in the crystal structure. However, predominant growth along the direction (002) does not occur. On the whole, similar behavior was seen by Jeon et al. [8], who reported that the crystallite diameter and the intensity of the (100) peak relative to the (002) peak increases with increasing temperature. We again note that the calculated crystallite

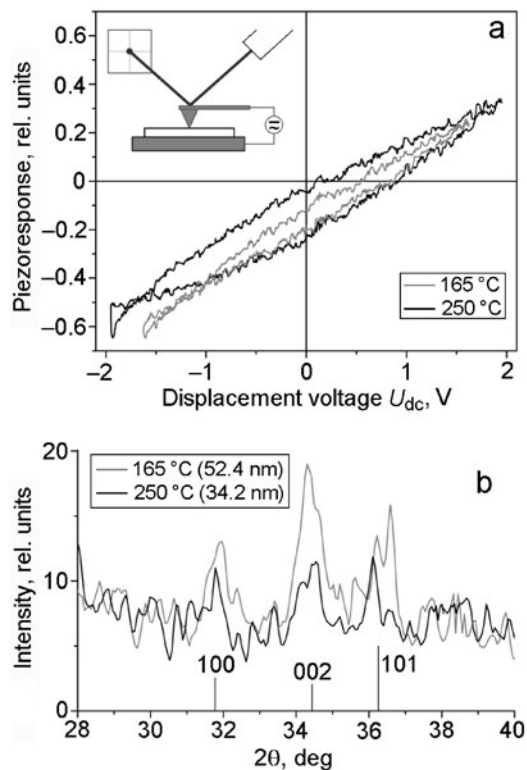


Fig. 3. Hysteresis loops of the piezoresponse (a) and X-ray spectra (b) of ZnO films grown at ALD reaction temperatures 165 °C (gray curves) and 250 °C (black curves). The insert in (a) demonstrates the PFM principle. The vertical black lines in (b) show the positions of the X-ray diffraction maxima for ZnO.

diameter in the case of reaction temperature 250 °C is virtually equal to the film thickness and may potentially be greater with an increased number of cycles and, as a result, greater magnitude of the piezoresponse.

These findings show that the structural and piezoelectric properties of thin ZnO films grown by atomic layer deposition depend on the reaction temperature. Despite the reduced contribution of the piezoactive (002) direction and increased conductance, ZnO films grown at higher base temperature have greater residual polarization. Thus, the piezoresponse for thin polycrystalline ZnO films obtained using atomic layer deposition is mainly a function of the microcrystalline nature of the film in the direction perpendicular to the plane of the base and the size of the ZnO grains.

As noted above, the ALD method is favorable for the stoichiometric growth of films with few defects and, as a consequence, low conductance [7]. Indeed, Table 1 shows that the ZnO films obtained have rather high resistance, which permits their use as coatings for transducers of surface acoustic waves (SAW). In order to explore the feasibility of using the films obtained as the sensitive element to the vapor of volatile organic compounds, we prepared and characterized SAW devices.

We prepared 100-nm-thick aluminum films on previously purified LiNbO₃ plates (Y-cut) by magnetic spraying in an argon atmosphere (Sputter Oxford). Interdigital transducers were prepared using standard photolithography and etching of the aluminum film in a solution of H₃PO₄ and HNO₃. Preliminary measurements of the conductance of ultrathin ZnO films showed that these films are virtually nonconducting ($R > 100 \text{ M}\Omega$) up to thickness 15-20 nm (100 ALD cycles for the given reaction temperatures). Thus, 8-nm-thick ZnO films were deposited at reaction temperature 165 °C on the surface of the devices in order to avoid short-circuiting the aluminum transducers (Fig. 4a).

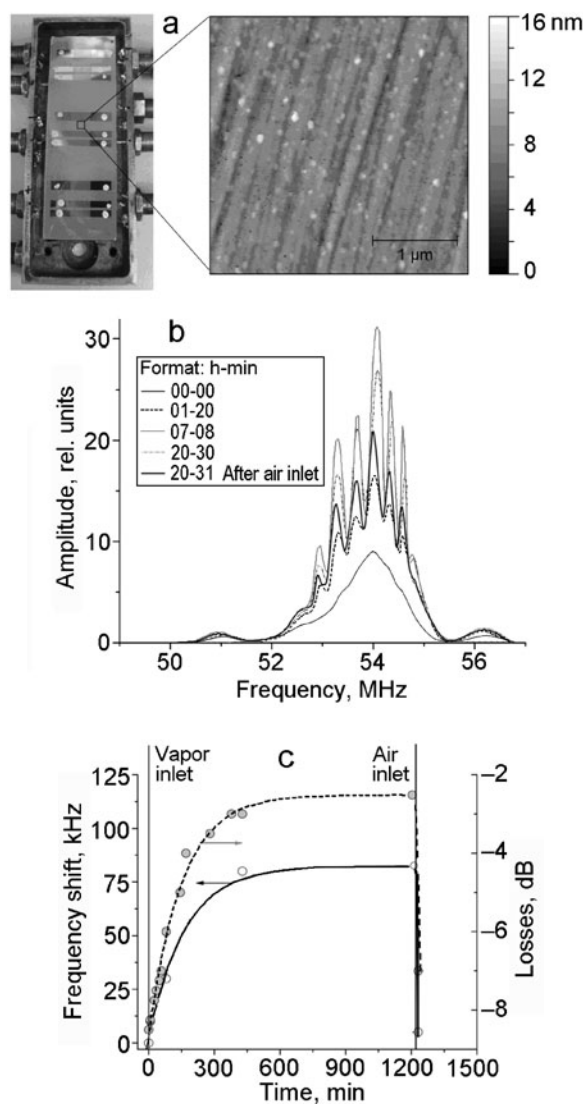


Fig. 4. a) Image of ZnO/LiNbO₃ SAW transducer and topography of the surface of a ZnO film obtained using ALD, b) AFC of the transducer over indicated time periods upon exposure to ethanol vapor, c) dependence of the position of the AFC peak and acoustic losses in the transducer on elapsed time.

The ZnO/LiNbO₃ SAW devices demonstrate acoustic losses of 8.5 dB at frequency 54 MHz (64 μm working wavelength) and room temperature in the air (Fig. 4b). Considerable changes in the amplitude–frequency characteristics (AFC) of the transducers are noted, namely, shape alteration, reduced losses, and a shift in the peak toward higher frequencies (Fig. 4b,c). The AFC of the transducers with a ZnO film in the presence of ethanol vapor are similar in shape to the characteristics of transducers without film (these results are not presented), i.e., the load on the acoustic transducer diminishes with increased time of exposure of the film in ethanol vapor. This finding suggests an effect of the variable viscoelastic properties of the film on the AFC. We note that the changes in the AFC related to the interaction of ethanol vapor with the film occur rather slowly (over several hours). The reverse process upon the inlet of pure air takes place much more rapidly (over a few seconds) and the AFC virtually return to the initial values. Furthermore, the process becomes completely reversible after heating of the films at 60 °C for 10 min.

The behavior of thin-film ZnO coatings on the surface of SAW transducers is primarily due to its structure, specifically, the circumstance that intercrystalline barriers permeate the film over its entire thickness. As a result, any changes in the intercrystalline space lead to a breakdown in the structural integrity of the film and to change in its viscoelastic properties. As a result of capillary condensation of ethyl alcohol in the intercrystalline contact areas and related chemical transformations, the film, “rigid” in its initial state, acquires the capacity for intercrystalline displacements, converting to an interdigitalized set of monocrystal fragments. Another factor may be chemical reactions in the region of the intercrystalline boundaries, where residues of unreacted diethylzinc on the crystallite surface in the presence of condensed ethanol are capable of forming complex compounds by analogy to reactions (1) and (2). The presence of diethylzinc in the film was confirmed by Raman spectroscopy using an NT-MDT Ntegra Spectra instrument. The Raman spectra of the films show peaks at 438 and 486 cm^{-1} (these data are not shown), which may be assigned to the E_2^{high} ZnO phonon mode [15] and Zn—C stretching vibrations of the diethylzinc molecule [16], respectively.

Our results demonstrate promise for the use of atomic layer deposition technology for growing nanometric films with given properties and the use of these films for the preparation of piezoelectric micromanipulators, acoustic transducers, or a broad range of sensor elements.

The authors thank S. Kravchenko at the V. E. Lashkaryov Institute of Semiconductor Physics of the National Academy of Sciences of Ukraine for a useful discussion and to the Seventh Framework Program of the European Union (EU Grant FP7 NANOMAT) for financial support.

REFERENCES

1. U. Ozgur, Y. I. Alivov, C. Liu, et al., *J. Appl. Phys.*, **98**, 041301 (2005).
2. S. J. Pearton, D. P. Norton, K. Ip, et al., *Progr. Mater. Sci.*, **50**, 293-340 (2005).
3. Z. L. Wang, *J. Phys.: Condens. Matter*, **16**, R829-R858 (2004).
4. T. Nagase, T. Kamohara, K. Nishikubo, et al., *J. Appl. Phys.*, **110**, 114120 (2011).
5. R. L. Puurunen, *J. Appl. Phys.*, **97**, 121301 (2005).
6. S. M. George, *Chem. Rev.*, **110**, 111-131 (2010).
7. E. Guziewicz, M. Godlewski, L. Wachnicki, et al., *Semicond. Sci. Technol.*, **27**, 074011 (2012).
8. S. Jeon, S. Bang, S. Lee, et al., *J. Electrochem. Soc.*, **155**, H738-H743 (2008).
9. H. Makino, A. Miyake, T. Yamada, et al., *Thin Solid Films*, **517**, 3138-3142 (2009).
10. L. Lutterotti, *Nucl. Instrum. Methods Phys. Res. B*, **268**, 334-340 (2010).
11. M. Alexe and A. Gruverman, *Nanoscale Characterisation of Ferroelectric Materials: Scanning Probe Microscopy Approach*, Springer, Berlin (2004).
12. S. V. Kalinin, A. N. Morozovska, L. Q. Chen, et al., *Rep. Prog. Phys.*, **73**, 056502 (2010).
13. A. Ulcinas, M. Es-Souni, and V. Snitka, *Sensors Actuators B*, **109**, 97-101 (2005).
14. A. V. Ankudinov and A. N. Titkov, *Phys. Solid State*, **47**, 1110-1117 (2005).
15. J. Z. Wang, M. Peres, J. Soares, et al., *J. Phys. Condens. Matter*, **17**, 1719-1724 (2005).
16. Y. S. Kim, Y. S. Won, H. Hagelin-Weaver, et al., *J. Phys. Chem. A*, **112**, 4246-4253 (2008).